http://dx.doi.org/10.12785/src/1570967474

Artificial Neural Networks for Strength Prediction of Fly Ash-based 3D-Printed Cementitious Materials

Marsail Al Salaheen
Department of Civil and Environmental Engineering
Universiti Teknologi PETRONAS
Seri Iskandar, Perak, Malaysia
marsail_20001253@utp.edu.my
Department of Civil and Environmental Engineering
Al-Husun University College, Al-Balqa Applied University
Irbid, Jordan
marsail.salaheen@bau.edu.jo

Wesam Salah Alaloul
Department of Civil and Environmental Engineering
Universiti Teknologi PETRONAS
Seri Iskandar, Perak, Malaysia
wesam.alaloul@utp.edu.my

Khalid Mhmoud Alzubi
Department of Civil and Environmental Engineering
Universiti Teknologi PETRONAS
Seri Iskandar, Perak, Malaysia
khalid_20001254@utp.edu.my
Department of Civil and Environmental Engineering
Al-Husun University College, Al-Balqa Applied University
Irbid, Jordan
alzoubi_khalid@bau.edu.jo

Muhammad Ali Musarat
Department of Civil and Environmental Engineering
Offshore Engineering Centre, Institute of Autonomous System
Universiti Teknologi PETRONAS
Seri Iskandar, Perak, Malaysia
ali.musarat@utp.edu.my

***Abstract*— This methodology employs Artificial Neural Networks (ANN) to predict the compressive strength of 3D-printed alkali-activated geopolymers, focusing on materials containing fly ash (FA). Data for training is gathered through an extensive literature review, encompassing parameters relevant to FA-containing geopolymers. After meticulous curation, a dataset of 53 experimental records, including mix ratios, chemical data, and 28-day compressive strength, is assembled. ANN architecture determination involves trial and error, considering different neurons and hidden layers, and various training algorithms. Results reveal that Levenberg Marquardt (*LM*) models consistently exhibit lower Mean Square Error (*MSE*), signifying superior accuracy. The best-performing LM model (7-11-1) outperforms Bayesian Regularization (*BR*) and Scaled Conjugate Gradient (*SCG*) models. The ANN achieves optimal validation performance offering a reliable framework for predicting 3D-printed material strength and enhancing construction material performance through understanding input parameter interplay.**

Keywords—3D Printing, ANN, compressive strength, fly ash, slag.

I. Introduction

3D printing technology for concrete presents numerous benefits in the field of construction. Primarily, it mitigates the demand for manual labor, reduces construction duration, and minimizes material inefficiency, thereby resulting in cost reductions and heightened efficacy [1]. Furthermore, it facilitates the creation of bespoke and environmentally friendly concrete components, thus contributing to the preservation of the environment [2]. This technology also allows to produce personalized structures, effectively diminishing the necessity for conventional design limitations [3]. Moreover, 3D printing in construction has the potential to bolster safety measures by diminishing the requirement for on-site construction activities [4].

Concrete 3D printing improves the sustainability of building projects by reducing material waste, lowering energy usage, and utilizing locally accessible resources [5]. The 3D printing carbon footprint can be reduced through the supplementary cementitious materials (SCM) as replacements for cement [6]. Because of aluminosilicates, geopolymers are suitable replacement to ordinary Portland cement (OPC). Each substance is made up of phases that contain silica and alumina, making them appropriate for geopolymer synthesis. Aluminosilicates found in industrial by-products such as (e.g., kaolinite, illite, fly ash (FA), red mud, steel slag, etc.) [7]. At either ambient or heated temperatures, geopolymers can be generated by a chemical reaction between aluminosilicate and silica components in an alkaline activator [8]. Geopolymers, do not rely on calcium carbonate as a major component, resulting in much fewer CO_2 emissions throughout the manufacturing process [9], [10]. As a result of its accessibility, energy efficiency, friendly manufacturing method, mechanical qualities, and durability, geopolymer cement has recently received a lot of attention [11]. The use of FA enhances the workability of the concrete, reduces permeability, and lowers the heat of cement hydration [12], [13]. It also improves the mechanical behavior of samples [14]. Furthermore, the small particle size of FA enhances the pores order of the concrete mix, limiting moisture infiltration and mitigating the impact of environmental attacks [11]. FA in 3D concrete printing can optimize silicate composite properties, boost buildability, and improve flexural tensile strength while decreasing volumetric weight [9]. The environmental effect of concrete manufacturing may be minimized by integrating FA, making it a more sustainable alternative.

The difficulties of employing 3D concrete printing for the building include material, strength, and printer setup limits [3]. These difficulties may be solved by using appropriate materials and improving printing settings to address concerns including workability, hardening time, and mechanical qualities [15]. strength performances and long-term behaviors are usual issues in 3D concrete printing [16]. Lack of technology, material variability, and optimization process are all obstacles to the advancement of 3D printing technology for concrete [4]. Similarly, the variety of non-standardized concrete details and the difficulties in creating complicated forms [17]. In addition, investigating the inherent correlation between the aforementioned factors and the mechanical efficacy of 3D printing through experimental means proves to be financially burdensome and time-consuming. One feasible resolution involves employing data-driven methodologies such as machine learning (ML) to prognosticate the performance of 3D printing based on the provided factors and divulge their underlying relationship.

Compressive strength is an essential characteristic of concrete, and it is commonly used to estimate other qualities; nonetheless, design of concrete buildings is primarily dependent on compressive strength. Several studies have investigated the impact of 3D printing on the compressive strength of FA-based materials for construction. FA is utilized in alkali-activated mixes for 3D printing to improve buildability and form preservation by affecting the mixture's yield stress, viscosity, and thixotropic buildup [18]. The inclusion of fly ash as a binder in concrete resulted in a compressive strength of 45MPa and a 15% reduction in water absorption [19]. Another study found that the best FA replacement level for high compressive strength was between 15% and 30%, whereas the best bond strength was reached with 10% to 15% fly ash [20]. At high levels, lengthy set periods and delayed strength development can lead to poor early-age strengths, which can be remedied by introducing steel slag [21]. These differences are mostly attributable to that the compressive strength of materials containing FA is affected by a number of parameters, including the water-to-cementitious materials ratio, the chemical composition of FA, its pozzolanic activity, the amount of FA replacement, and the mixing design.

The evaluation of the dependence of compressive strength on each specific factor requires the use of intricate mathematical computations, which have been successfully addressed due to the implementation of computer systems. One of the computational techniques utilized to ascertain the comprehensive correlation between plentiful and intricate data is the artificial neural network (ANN). An ANN possesses the capability to replicate virtually any complicated association between the inputs and outputs [22], [23]. The effective parameters on the compressive strength of 3D printed materials are estimated by the neural network through utilization of the findings obtained in prior experiments. Consequently, the network possesses the capability to predict the anticipated output with a certain degree of error, provided that its input parameters are available [24]. The development of accurate and dependable models for predicting the compressive strength of 3D printing materials can result in significant time and cost savings. Hence, the precise and preliminary estimation of the durability of the 3D printed strength materials holds great significance within construction materials.

Many investigations have been undertaken utilizing artificial intelligence (AI) to explore the effect of SCM on the mechanical characteristics of conventional concrete. However, a thorough investigation is required to assess the influence of SCM features on the mechanical properties of 3D-printed building materials. Although it has been established that the characteristics of SCM have an impact on various attributes of 3D printed materials, little study has been conducted to determine the amount to which each character is significant and its relative importance.

The objective of this investigation is to ascertain the compressive strength of cementitious materials that have been 3D printed and incorporate FA. This was achieved through the utilization of an ANN that employs a backpropagation algorithm. Furthermore, the study considers the various physical and chemical attributes that impact compressive strength. The limitations encountered during the experimental testing phase were successfully addressed by incorporating a multitude of datasets that possess diverse properties as input for the ANN. Consequently, this study furnishes methodologies for effectively implementing neural networks in the field of engineering. In addition, a soft computing technique is employed to extrapolate the findings garnered from the collected data to novel and unfamiliar scenarios.

II. Methodology

A. Development of the artificial neural network

The ANN is made up of interconnected processing pieces called neurons or nodes that are intended to solve certain challenges. The ANN training procedure is separated into two stages: learning and testing. During the learning phase, the network's real information is entered, allowing the networks to gain the capacity to calculate the intended results through iterative learning. In this work, the ANN models and compressive strength of 3D-printed alkali-activated geopolymers were predicted using MATLAB software version 9.14.0 (R2023a). The sample's training component is based on the feed-forward backpropagation learning technique to find the top model capable of producing a reliable forecast.

B. Dataset

To initiate the construction of an ANN, the first step entails formulating the various parameters involved in the 3D printing of alkali-activated geopolymers containing FA. To collect these parameters, a comprehensive and systematic examination of existing literature was conducted. This involved putting a specific sequence of keywords into a research engine, which yielded a range of different papers. In this case, the research utilized the Scopus database with "TITLE-ABS-KEY ((mix OR details) AND (3d) AND (print*) AND (Fly ash OR waste-based OR recycled materials).) AND PUBYEAR > 2017 AND PUBYEAR < 2024", from which a total of forty papers were gathered.

The primary objective of developing this database was to accumulate experimental data that could be utilized to train the ANN and generate predictions. Consequently, certain papers were excluded from the collection due to their lack of experimental data or insufficient information. For instance, papers that omitted crucial details, such as the water-binder ratio, which is undeniably one of the most critical parameters in any mixture design, were disregarded. Similarly, papers that did not provide pertinent information in this regard were also omitted, to increase the dataset some results from related papers have been added. This results in the creation of a database of publications (47 in all) from which the parameters are calculated.

Utilizing a back propagation neural network approach, models were constructed using a total of 53 experimental datasets [25]–[41]. The compressive strength of 3D-printed concrete containing FA has been estimated using previously reported results. The dataset compiled for this purpose included information about the mix composition ratio of FA, slag, water, and aggregates. In addition, the inputs considered were the CaO, SiO_2, and Al_2O_3 content, as FA exhibits varying chemical and physical characteristics depending on its type and source. The curing age of samples was also included in the dataset. The collection was built using data from research investigations that offered specific information regarding concrete mix proportions, FA chemical composition, and 3D printed structures compressive strength at 28-days. Table I contains a summary of the input and output parameters.

TABLE I. INPUT AND OUTPUT PARAMETERS FOR THE ANN MODELS

Input Parameters	Output Parameter
FA: b	28 Days Compressive Strength
S: b	
W: b	
A: b	
SiO_2	
Al_2O_3	
CaO	

[a] FA: fly ash; b: binder; S: slag; W: water; A: aggregate.

The dataset was carefully curated to constitute a reasonably inclusive assemblage Including all of the critical factors that determine the behavior of FA in 3D printed concrete. Statistical parameters for the dataset are displayed in Table II and have the potential to offer a broad overview of the mixture proportions employed.

TABLE II. STATISTICAL PARAMETERS FOR THE DATASET.

Parameter	Min	Max	mean	SD
FA: b	0.0	1.00	0.56	0.36
S: b	0.0	1.00	0.11	0.20
W: b	0.13	2.01	0.48	0.35
A: b	0.3	4.00	1.20	0.56
SiO_2	15.00	65.6	50.59	8.18
Al_2O_3	15.00	39.35	26.15	5.70
CaO	1.21	25.97	6.68	5.66
Compressive Strength	4.14	55.2	32.99	15.29

C. Modeling the network

The identification of the most suitable arrangement of the network, which can yield both a well-established and highly precise result, holds significant importance. Different structures with varying numbers of neurons in each layer were investigated. The network's mean square error (MSE) and R-value were computed for every neuron quantity in the hidden layer.

The current study thoroughly examined and utilized various training techniques, such as Levenberg Marquardt (LM), Bayesian Regularization (BR), and Scaled Conjugate Gradient (SCG), to enhance the architecture of the ANN. The LM algorithm is widely employed for optimizing the training process of ANNs. This algorithm integrates components of both the gradient descent and Gauss-Newton methods, dynamically adjusting the learning rate to achieve efficient convergence. BR incorporates Bayesian principles to regularize the network, preventing overfitting by assigning probability distributions to the model's parameters. This probabilistic approach establishes a framework to strike a balance between model complexity and data fitting. On the other hand, SCG is an iterative optimization algorithm that effectively minimizes the error function by adapting the step size based on the curvature of the error surface. SCG is particularly useful in training ANNs when the computation of the matrix is computationally expensive. Each of these algorithms provides a distinct approach to addressing the challenges encountered in the training of neural networks, allowing researchers and practitioners to select the most suitable option based on their specific requirements and data characteristics. For the ANN's hidden and output layers, a sigmoid transfer function was applied.

III. RESULT AND DISCUSSION

A. ANN Performance

Different numbers of neurons (8, 9, 10, 11, and 12) were implemented in the concealed layer of the three examined training algorithms throughout the training procedure, while the number of neurons in the input layer stayed consistent at seven. In the testing stage, the suitable quantity of neurons in the concealed layer was ascertained based on the lowest MSE and highest efficacy; the neural models are presented in Table III.

TABLE III. STATISTICAL VALUES OF ANN MODELS.

Training, Testing and Validation Stage			
Algorithm	*MSE*	*$R_{(Train)}$*	*$R_{(All)}$*
LM (7-8-1)	0.0086	0.9489	0.95244
LM (7-9-1)	0.0076	0.9545	0.94718
LM (7-10-1)	0.0075	0.9507	0.93776
LM (7-11-1)*	0.0073	0.9558	0.95673
LM (7-12-1)	0.0087	0.9514	0.94085
BR (7-8-1)	0.0089	0.9509	0.94386
BR (7-9-1)	0.0085	0.9503	0.95156
BR (7-10-1)	0.0092	0.9439	0.94917
BR (7-11-1)	0.0084	0.9537	0.95288
BR (7-12-1)	0.0083	0.9499	0.95010
SCG (7-8-1)	0.0153	0.9110	0.90460
SCG (7-9-1)	0.0097	0.9372	0.92125

SCG (7-10-1)	0.0117	0.9300	0.93796
SCG (7-11-1)	0.0159	0.9112	0.91107
SCG (7-12-1)	0.0155	0.9011	0.90163

It is evident that the LM models consistently demonstrate lower MSE values, indicating a superior level of predictive accuracy when compared to both the BR and SCG models. These findings deserve special attention since they correspond with the discoveries outlined in the current body of research. It represents a reliable option for enhancing the performance of neural network models due to their favorable convergence properties, exceptional accuracy, and reduced temporal demands [42]. The LM (7-11-1) model stands out with the lowest MSE, highlighting its prowess as the top-performing model in minimizing predictive errors. Furthermore, the BR (7-11-1) model also showcases a low MSE, positioning it as one of the more proficient BR models.

On the other hand, the SCG models generally exhibit higher MSE values, suggesting a less precise fit to the data in comparison to the LM and BR models. Although SCG (7-9-1) records the lowest MSE among the SCG models, it still falls short of matching the performance of the best-performing LM and BR models.

The predictive ability of compressive strength for 3D construction materials incorporating FA can be ascertained upon successful training of the network. Moreover, the intricate relationship among the input parameters can be elucidated by means of the network. Fig. 1 depicts an evaluation of the networks' effectiveness in calculating compressive strength. The best validation performance was obtained in the 12th epoch, with a value of 0.00890.

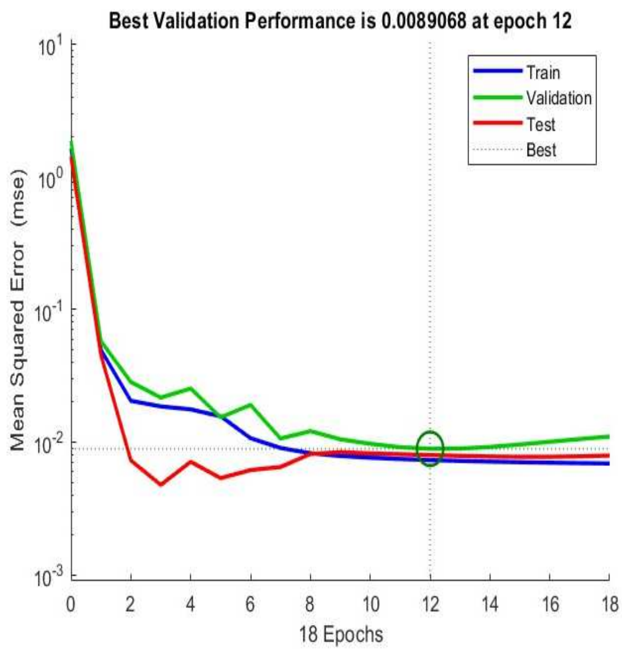

Fig. 1. The performance of the optimal network.

Fig. 2 depicts the estimation quality as a function of R for all data, demonstrating the relationship between the experimental result and the ANN model output. It clearly displays total dataset response with R confirming that the network computed the data accurately.

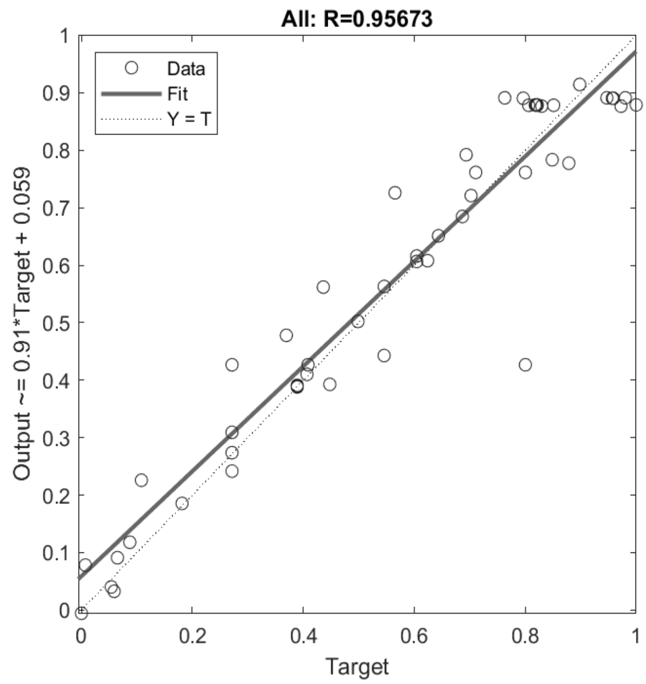

Fig. 2. The regression of the optimal network.

Fig. 3 depicts a comparison of the findings for the compressive strength of FA-based samples made by 3D printing with the projected outcomes derived from the ANN. It is evident that the networks were able to forecast the experimental results with a commendable level of precision, which is deemed appropriate for practical applications.

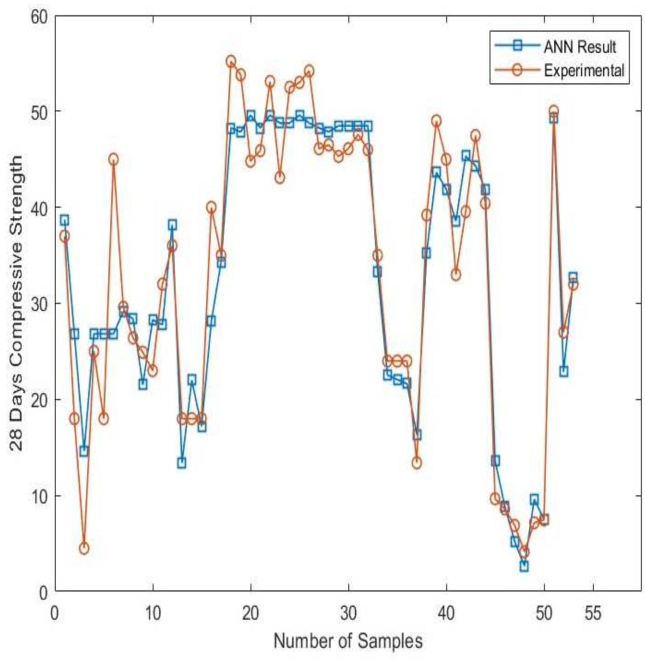

Fig. 3. The comparison between predicted and experimental results.

B. Sensitivity Analysis

Garson's factor, also referred to as Garson's algorithm, is a methodology employed to evaluate the comparative significance of input factors or independent variables in a neural network model. This technique aids researchers and data scientists in comprehending which factors possess the most substantial impact on the predictions or outcomes of the model. The application of Garson's factor analysis is primarily confined to neural networks that encompass at least a single hidden layer. It assesses the significance of each input factor by scrutinizing the connection weights within the network.

The resultant Garson's factors offer valuable insights into the relative importance of each input factor in influencing the output of the neural network. Higher Garson's factors signify greater importance, whereas lower factors imply lesser influence. The results for the proposed model plotted in Fig. 4.

In this context, the labels and weights appear to represent the factors and their importance in the model. The weight of 0.18 of S: b indicates that variations in slag content have a relatively high impact on the model's predictions. S: b content is a key factor affecting the model's outcome standing with FA: b, CaO and W: b with 0.17, 0.16 and 0.15 weights respectively.

In summary, these findings indicate the relative relevance of various input parameters in the neural network model. The specific interpretation of A: b and Al_2O_3 may require additional context in influencing the model's predictions, as indicated by their lower weights.

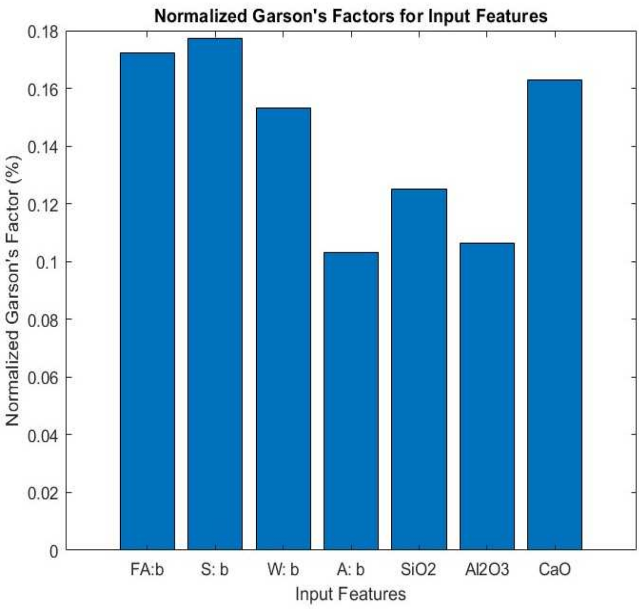

Fig. 4. Feature importance for the model parameters.

IV. CONCLUSION

Estimating the compressive strength of 3D printed materials including FA using an ANN model that considers both ease and precision will help to save time, energy, and money. To be used in the ANN model, a comprehensive collection of 53 independent experimental records of FA-based alkali-activated 3D printed materials was compiled from the literature. The subsequent inferences were concluded subsequent to examining the suggested ANN model:

- The networks show high precision in predicting with an MSE lower than 0.008 for the LM-trained algorithm with R around 0.95.
- The results of feature importance show that S: b, CaO, FA: b and W: b are the most crucial variables for predicting the compressive strength of 3D printed materials containing alkali-activated FA.

However, the data in this study were obtained from preexisting literature. The experimental conditions varied among the articles, and the dataset was restricted. In order to obtain more dependable models, controlled experimental trials need to be carried out, and data must be collected from a singular source in accordance with the prevailing environmental conditions. Also, developing empirical equations to predict is of interest.

ACKNOWLEDGMENT

The authors would like to thank Universiti Teknologi PETRONAS and University of Bahrain for the support provided in this research.

REFERENCES

[1] N. O. E. Olsson, E. Arica, R. Woods, and J. A. Madrid, “Industry 4.0 in a project context: Introducing 3D printing in construction projects,” *Project Leadership and Society*, vol. 2, p. 100033, Dec. 2021, doi: 10.1016/j.plas.2021.100033.

[2] A. Hunbus and B. AlMangour, “A Critical Review of Construction Using 3D Printing Technology,” *ASME Journal of Engineering for Sustainable Buildings and Cities*, vol. 4, no. 020801, Jul. 2023, doi: 10.1115/1.4062730.

[3] T. Tabassum and A. Ahmad Mir, “A review of 3d printing technology-the future of sustainable construction,” *Materials Today: Proceedings*, Aug. 2023, doi: 10.1016/j.matpr.2023.08.013.

[4] P. B.a, L. N, A. Buradi, S. N, P. B l, and V. R, “A comprehensive review of emerging additive manufacturing (3D printing technology): Methods, materials, applications, challenges, trends and future potential,” *Materials Today: Proceedings*, vol. 52, pp. 1309–1313, Jan. 2022, doi: 10.1016/j.matpr.2021.11.059.

[5] Y. Tarhan, F. Craveiro, and H. Bartolo, “An Overview of Binder Materials’ Sustainability for 3D Printing in Construction,” in *Progress in Digital and Physical Manufacturing*, J. O. Correia Vasco, H. de Amorim Almeida, A. Gonçalves Rodrigues Marto, C. A. Bento Capela, F. G. da Silva Craveiro, H. M. Coelho da Rocha Terreiro Galha Bártolo, L. M. de Jesus Coelho, M. A. Simões Correia, M. M. Nogueira Vieira, and R. M. Barreiros Ruben, Eds., in Springer Tracts in Additive Manufacturing. Cham: Springer International Publishing, 2023, pp. 291–302. doi: 10.1007/978-3-031-33890-8_26.

[6] A. Motalebi, M. A. H. Khondoker, and G. Kabir, “A Systematic Review of Life Cycle Assessments of 3D Concrete Printing,” *Sustainable Operations and Computers*, Aug. 2023, doi: 10.1016/j.susoc.2023.08.003.

[7] S. Al-Qutaifi, A. Nazari, and A. Bagheri, “Mechanical properties of layered geopolymer structures applicable in concrete 3D-printing,” *Construction and Building Materials*, vol. 176, pp. 690–699, Jul. 2018, doi: 10.1016/j.conbuildmat.2018.04.195.

[8] J. L. Provis and J. S. J. van Deventer, *Geopolymers: Structures, Processing, Properties and Industrial Applications*. Elsevier, 2009.

[9] D. K. Nayak, P. P. Abhilash, R. Singh, R. Kumar, and V. Kumar, “Fly ash for sustainable construction: A review of fly ash concrete and its beneficial use case studies,” *Cleaner Materials*, vol. 6, p. 100143, Dec. 2022, doi: 10.1016/j.clema.2022.100143.

[10] M. Al Salaheen, W. S. Alaloul, K. M. Alzubi, A. bahaa A. Malkawi, and M. A. Musarat, “Advancing waste-based construction materials through carbon dioxide curing: A comprehensive review,” *Results in Engineering*, vol. 20, p. 101591, Dec. 2023, doi: 10.1016/j.rineng.2023.101591.

[11] J.-L. Tao, C. Lin, Q.-L. Luo, W.-J. Long, S.-Y. Zheng, and C.-Y. Hong, “Leveraging internal curing effect of fly ash cenosphere for alleviating autogenous shrinkage in 3D printing,” *Construction and Building Materials*, vol. 346, p. 128247, Sep. 2022, doi: 10.1016/j.conbuildmat.2022.128247.

[12] M. Ashfaq and A. Moghal, “Cost and Carbon Footprint Analysis of Flyash Utilization in Earthworks,” *International Journal of Geosynthetics and Ground Engineering*, Apr. 2022, doi: 10.1007/s40891-022-00364-4.

[13] M. Al Salaheen *et al.*, “Modelling and Optimization for Mortar Compressive Strength Incorporating Heat-Treated Fly Oil Shale Ash as an Effective Supplementary Cementitious Material Using Response Surface Methodology,” *Materials*, vol. 15, no. 19, Art. no. 19, Jan. 2022, doi: 10.3390/ma15196538.

[14] M. Ahmaruzzaman, “A review on the utilization of fly ash,” *Progress in Energy and Combustion Science*, vol. 36, no. 3, pp. 327–363, Jun. 2010, doi: 10.1016/j.pecs.2009.11.003.

[15] P. S. Ambily, S. K. Kaliyavaradhan, and N. Rajendran, “Top challenges to widespread 3D concrete printing (3DCP) adoption – A review,” *European Journal of Environmental and Civil Engineering*, vol. 0, no. 0, pp. 1–29, 2023, doi: 10.1080/19648189.2023.2213294.

[16] P. Bedarf, C. Calvo-Barentin, D. M. Schulte, A. Şenol, E. Jeoffroy, and B. Dillenburger, “Mineral composites: stay-in-place formwork for concrete using foam 3D printing,” *Archit. Struct. Constr.*, vol. 3, no. 2, pp. 251–262, Jun. 2023, doi: 10.1007/s44150-023-00084-x.

[17] A. Tamimi, H. Alqamish, A. Khaldoune, H. Alhaidary, and K. Shirvanimoghaddam, “Framework of 3D Concrete Printing Potential and Challenges,” *Buildings*, vol. 13, p. 827, Mar. 2023, doi: 10.3390/buildings13030827.

[18] P. Paiste, M. Liira, I. Heinmaa, S. Vahur, and K. Kirsimäe, “Alkali activated construction materials: Assessing the alternative use for oil shale processing solid wastes,” *Construction and Building Materials*, vol. 122, pp. 458–464, Sep. 2016, doi: 10.1016/j.conbuildmat.2016.06.073.

[19] L. Dvorkin, J. Konkol, V. Marchuk, and A. Huts, “Effectiveness of Polymer Additives in Concrete for 3D Concrete Printing Using Fly Ash,” *Polymers*, vol. 14, no. 24, Art. no. 24, Jan. 2022, doi: 10.3390/polym14245467.

[20] N. Shafiq and A. Ammar, “An Experimental Assessment on the Performance of Fly Ash in Concrete,” 2021, pp. 458–467. doi: 10.1007/978-981-33-6311-3_53.

[21] W. Alaloul, M. Salaheen, A. Malkawi, K. alzu’bi, and M. A. Musarat, “Utilizing of oil shale ash as a construction material: A systematic review,” *Construction and Building Materials*, vol. 299, Jun. 2021, doi: 10.1016/j.conbuildmat.2021.123844.

[22] M. J. Moradi, M. Khaleghi, J. Salimi, V. Farhangi, and A. M. Ramezanianpour, “Predicting the compressive strength of concrete containing metakaolin with different properties using ANN,” *Measurement*, vol. 183, p. 109790, Oct. 2021, doi: 10.1016/j.measurement.2021.109790.

[23] J.-S. Chou, C.-F. Tsai, A.-D. Pham, and Y.-H. Lu, “Machine learning in concrete strength simulations: Multi-nation data analytics,” *Construction and Building Materials*, vol. 73, pp. 771–780, Dec. 2014, doi: 10.1016/j.conbuildmat.2014.09.054.

[24] N. Ganasen, L. Krishnaraj, K. C. Onyelowe, G. U. Alaneme, and O. N. Otu, “Soft computing techniques for predicting the properties of raw rice husk concrete bricks using regression-based machine learning approaches,” *Sci Rep*, vol. 13, no. 1, Art. no. 1, Sep. 2023, doi: 10.1038/s41598-023-41848-1.

[25] K. Korniejenko *et al.*, “A Comparative Study of Mechanical Properties of Fly Ash-Based Geopolymer Made by Casted and 3D Printing Methods,” *IOP Conf. Ser.: Mater. Sci. Eng.*, vol. 660, no. 1, p. 012005, Nov. 2019, doi: 10.1088/1757-899X/660/1/012005.

[26] B. Panda, S. C. Paul, L. J. Hui, Y. W. D. Tay, and M. J. Tan, “Additive manufacturing of geopolymer for sustainable built environment,” *Journal of Cleaner Production*, vol. 167, pp. 281–288, Nov. 2017, doi: 10.1016/j.jclepro.2017.08.165.

[27] B. Shantanu, J. Smrati, and S. Manu, “Criticality of binder-aggregate interaction for buildability of 3D printed concrete containing limestone calcined clay,” *Cement and Concrete Composites*, vol. 136, p. 104853, Feb. 2023, doi: 10.1016/j.cemconcomp.2022.104853.

[28] B. Panda, Y. w. d. Tay, S. c. Paul, and M. j. Tan, “Current challenges and future potential of 3D concrete printing,” *Materialwissenschaft und Werkstofftechnik*, vol. 49, no. 5, pp. 666–673, 2018, doi: 10.1002/mawe.201700279.

[29] D. Chaiyotha, W. Kantawong, P. Payakaniti, S. Pinitsoontorn, and P. Chindaprasirt, “Finding optimized conditions for 3D printed high calcium fly ash based alkali-activated mortar,” *Case Studies in Construction Materials*, vol. 18, p. e01976, Jul. 2023, doi: 10.1016/j.cscm.2023.e01976.

[30] J. Marczyk *et al.*, “Hybrid Materials Based on Fly Ash, Metakaolin, and Cement for 3D Printing,” *Materials*, vol. 14, no. 22, Art. no. 22, Jan. 2021, doi: 10.3390/ma14226874.

[31] B. Panda, S. Ruan, C. Unluer, and M. J. Tan, “Improving the 3D printability of high volume fly ash mixtures via the use of nano attapulgite clay,” *Composites Part B: Engineering*, vol. 165, pp. 75–83, May 2019, doi: 10.1016/j.compositesb.2018.11.109.

[32] T. Mukhametkaliyev, M. H. Ali, V. Kutugin, O. Savinova, and V. Vereschagin, “Influence of Mixing Order on the Synthesis of Geopolymer Concrete,” *Polymers*, vol. 14, no. 21, Art. no. 21, Jan. 2022, doi: 10.3390/polym14214777.

[33] H. Alghamdi, S. A. O. Nair, and N. Neithalath, “Insights into material design, extrusion rheology, and properties of 3D-printable alkali-activated fly ash-based binders,” *Materials & Design*, vol. 167, p. 107634, Apr. 2019, doi: 10.1016/j.matdes.2019.107634.

[34] B. Panda, C. Unluer, and M. J. Tan, “Investigation of the rheology and strength of geopolymer mixtures for extrusion-based 3D printing,” *Cement and Concrete Composites*, vol. 94, pp. 307–314, Nov. 2018, doi: 10.1016/j.cemconcomp.2018.10.002.

[35] B. Panda, S. C. Paul, N. A. N. Mohamed, Y. W. D. Tay, and M. J. Tan, “Measurement of tensile bond strength of 3D printed geopolymer mortar,” *Measurement*, vol. 113, pp. 108–116, Jan. 2018, doi: 10.1016/j.measurement.2017.08.051.

[36] P. Meloni, G. Carcangiu, and R. Licheri, “Mix Design of Geopolymeric Formulations for Environmentally Sustainable Structural Applications,” *Chemical Engineering Transactions*, vol. 100, pp. 403–408, Jun. 2023, doi: 10.3303/CET23100068.

[37] S. Kaushik, M. Sonebi, G. Amato, U. K. Das, and A. Perrot, “Optimisation of Mix Proportion of 3D Printable Mortar Based on Rheological Properties and Material Strength Using Factorial Design of Experiment,” *Materials*, vol. 16, no. 4, Art. no. 4, Jan. 2023, doi: 10.3390/ma16041748.

[38] J. Marczyk *et al.*, “Optimizing the L/S Ratio in Geopolymers for the Production of Large-Size Elements with 3D Printing Technology,” *Materials*, vol. 15, no. 9, Art. no. 9, Jan. 2022, doi: 10.3390/ma15093362.

[39] S. Volpe *et al.*, “Preparation and characterization of novel environmentally sustainable mortars based on magnesium potassium phosphate cement for additive manufacturing,” *AIMSMATES*, vol. 8, no. 4, Art. no. matersci-08-04-039, 2021, doi: 10.3934/matersci.2021039.

[40] M. Xia, B. Nematollahi, and J. Sanjayan, “Printability, accuracy and strength of geopolymer made using powder-based 3D printing for construction applications,” *Automation in Construction*, vol. 101, pp. 179–189, May 2019, doi: 10.1016/j.autcon.2019.01.013.

[41] B. Panda, G. B. Singh, C. Unluer, and M. J. Tan, “Synthesis and characterization of one-part geopolymers for extrusion based 3D concrete printing,” *Journal of Cleaner Production*, vol. 220, pp. 610–619, May 2019, doi: 10.1016/j.jclepro.2019.02.185.

[42] M. Hosseinpour, H. Sharifi, and Y. Sharifi, “Stepwise regression modeling for compressive strength assessment of mortar containing metakaolin,” *International Journal of Modelling and Simulation*, vol. 38, no. 4, pp. 207–215, 2018, doi: 10.1080/02286203.2017.1422096.